

# Combined Infrared and Raman temperature measurements on device structures

A. Sarua<sup>1</sup>, Hangfeng Ji<sup>1</sup>, M. Kuball<sup>1</sup>, M. J. Uren<sup>2</sup>, T. Martin<sup>2</sup>, K. P. Hilton<sup>2</sup>, and R. S. Balmer<sup>2</sup>

<sup>1</sup>H.H. Wills Physics Laboratory, University of Bristol, Tyndall Avenue, Bristol BS8 1TL, United Kingdom  
phone: +44 117 3317739 e-mail: a.sarua@bristol.ac.uk

<sup>2</sup>QinetiQ Ltd., St. Andrew's Road, Malvern, Worcs, WR14 3PS, United Kingdom

**Keywords:** HFET, GaN, Raman, Infrared, thermography, temperature

## Abstract

**Combined Infrared and micro-Raman techniques were applied to measure temperature rise in semiconductor device structures based on AlGaIn/GaN HFETs. Results from both techniques were compared and temperature and spatial resolution issues were discussed. Finite-difference 3D modeling of temperature distributions was performed to aid the interpretation of the experimental data. In addition the versatility of the Raman method was demonstrated for a GaAs pHEMT device.**

## INTRODUCTION

A demand for more higher frequency and higher power devices for use in radar and mobile communications has stimulated the research activity in the area of wide bandgap III-V semiconductor materials, such as GaN, AlN and their alloys. These materials can offer properties beyond the conventional semiconductor materials, such as excellent electron mobility, high breakdown voltage and high thermal conductivity. For instance AlGaIn/GaN HFET devices were reported to exhibit power densities as high as tens of Watt per mm [1]. Therefore, thermal management is an important aspect in the device package design, as significant heat generation occurs in the active area of these high-power devices. [2-4]

Although there are some well-established techniques to assess the temperature rise in operating devices like infrared (IR) thermography [5-8], there are key challenges related to the ever decreasing dimensions of recent devices. For example in AlGaIn/GaN power transistors heat is generated in a strip near the gate of less than 0.5 $\mu\text{m}$  width [2,3]. As a result the diffraction limited resolution of 2-5  $\mu\text{m}$  for IR light prevents accurate temperature monitoring using IR thermography. Raman spectroscopy together with the higher spatial resolution of optical microscopy has been reported to be able to obtain temperature of semiconductors in the micron or submicron resolution range.[2-5] However, this method is difficult to apply for measuring temperatures of metals and other materials, which do not have suitable phonon lines in their spectrum. Thus there is a need for a system which can provide coverage of different materials, high spatial resolution and fast measurement times. In this

work we demonstrate a combined Raman and IR imaging approach to retrieve the temperature of active devices.

## EXPERIMENTAL DETAILS

The devices used were 2x50  $\mu\text{m}$  AlGaIn/GaN HFET structures and consisted of 30 nm AlGaIn, 1.2  $\mu\text{m}$  of GaN on 300  $\mu\text{m}$  of 4H-SiC substrate. Standard Ti/Al/Pt/Au Ohmic contacts and Ni/Au Schottky gate contacts were used. Source-drain gap was 4.8  $\mu\text{m}$  and gate length was 1.2  $\mu\text{m}$ . The wafer was cut into large die which were mounted on a well thermally sunk package, with a 2 mm hole for optical access from below the device area. All electrical measurements were carried out under DC bias. Figure 1 shows the optical image of an AlGaIn/GaN HFET device, as seen through the transparent SiC substrate.

Infrared imaging measurements were carried out with a custom build Quantum Focus Instrument (QFI) Infrascopes system, equipped with LN<sub>2</sub>-cooled 256x256 InSb detector array. IR light was collected by a SiGe 15x (NA=0.5) objective lens, with working distance WD = 16 mm. Spatial resolution of the system is diffraction limited to about 5  $\mu\text{m}$  on the sample surface and pixel resolution of the infrared image is about 1.6  $\mu\text{m}$ . To acquire the infrared temperature a sample radiance calibration was performed, allowing pixel to pixel correction of the target emissivity. Once emissivity is obtained, temperature of the selected area can be retrieved almost instantly. Details of the IR thermography method are provided elsewhere [6,7].

This infrared system was integrated into the Leica microscope of a Renishaw InVia system, which was used to perform micro-Raman measurements. The 488 nm line of an Ar<sup>+</sup> ion laser was used as optical excitation source and the scattered signal was collected by a Peltier-cooled CCD detector. A 50x (NA=0.55) objective lens was used to focus the laser beam spot onto the sample surface with diameter of about 0.5-0.7  $\mu\text{m}$ . In confocal mode the depth of focus can be estimated as 1-2  $\mu\text{m}$ . Spectral resolution of the InVia system is 2  $\text{cm}^{-1}$ , and resolution in the shift is  $\pm 0.02 \text{ cm}^{-1}$ .

Raman and IR measurements were performed from the back side of the device, since SiC and GaN are transparent for the range of wavelengths used here (Fig. 1). As both infrared and visible objective lenses are mated to the same microscope turret, the switching between Raman and IR

mode can be easily achieved allowing quasi-simultaneous measurements. An XY-mapping stage with resolution of 0.1  $\mu\text{m}$  was used to obtain 2D scans of the device temperature. Temperature of the heat sink during measurements was kept at 25  $^{\circ}\text{C}$  using a Peltier heater stage.

For 3D thermal simulations a commercial TAS finite difference package was used. In simulations thermal conductivity of GaN was 160 W/mK and SiC 330 W/mK, and temperature dependence of the thermal conductivities was assumed to be  $1/T^n$ , where  $n$  was 1.4 for GaN and 1.5 for SiC.

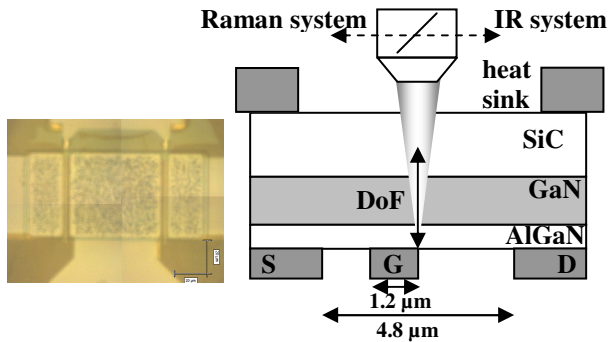


Figure 1. Optical image of  $2 \times 50 \mu\text{m}$  finger AlGaIn/GaN HFET through the SiC substrate (left). Outline of the HFET device structure and experimental set-up (right).

## EXPERIMENTAL RESULTS

The result of the IR temperature measurements for AlGaIn/GaN HFET is shown on Fig. 2a, with source-drain bias ( $V_{sd}$ ) of 40V applied to just one of the two fingers. A hot spot in the vicinity of the source-drain gap was observed with peak temperature of about 114  $^{\circ}\text{C}$ . The areas with metal contacts away from the channel show a temperature of about 60  $^{\circ}\text{C}$ , while in areas where no metal is covering the surface a temperature of 27  $^{\circ}\text{C}$  was measured by IR thermography.

2D Raman temperature measurements were carried out over the active finger area of the same HFET, shown in the Fig. 2a by a dashed rectangle. Temperature of GaN was determined from the temperature dependence of the  $E_2(\text{high})$  phonon mode of GaN. Since depth of the focus is on order of 1-2  $\mu\text{m}$  (Fig. 1) measurement averages the temperature over the thickness of the GaN layer (1.2  $\mu\text{m}$ ). Details of the measurement technique have been described elsewhere [2-4]. A pinched-off state of the device was used here as reference for temperature determination to compensate for the possible piezoelectric contributions.

Raman measurements showed higher peak temperatures of GaN in the source-drain gap of about 160  $^{\circ}\text{C}$ , but temperatures away from the source-drain region are close to IR temperatures (Fig 2). The Raman measurements showed that edge of the chip had a temperature of 42  $^{\circ}\text{C}$ , while the heat sink was kept at 25  $^{\circ}\text{C}$  by the Peltier stage.

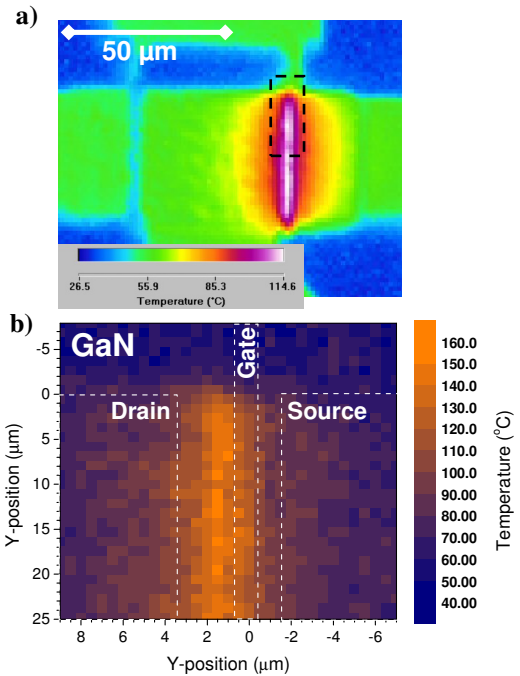


Figure 2. a) IR temperature map of AlGaIn/GaN HFET device at  $V_{sd} = 40\text{V}$  and  $I = 25 \text{ mA}$ . b) Map of GaN temperature at the same power over selected area shown by rectangle in a).

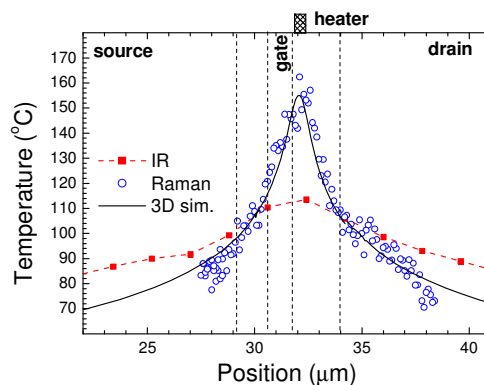


Figure 3. Line temperature profiles recorded by IR and Raman systems in the source-drain gap of the operated AlGaIn/GaN HFET device. Simulated temperature profile for the average GaN temperature (solid line). Position of the heater is also displayed.

Figure 3 shows the line profile of the device temperature as measured in the middle of the operating HFET finger by Raman and IR techniques. The IR technique shows the same location of the hot spot but a lower peak temperature in the channel and a much broader width of temperature profile, than obtained in the Raman measurement.

3D finite difference simulations were performed and the result for average temperature in the GaN layer is displayed in Fig. 3. The dissipated power was the same as in the experiment and a heater with length of 0.5  $\mu\text{m}$  was placed on the AlGaIn/GaN interface in the gate-drain gap close to the

gate edge (Fig. 3). Good agreement with the Raman temperature profile was achieved.

## DISCUSSION

In the following we compare the results of IR and Raman techniques obtained on AlGaIn/GaN HFET devices in order to underline their relative advantages and limitations and illustrate the benefit of a combined approach. As the size of the source-drain openings in these devices is only 4.8 microns the results of IR thermography are affected by diffraction limited resolution effects. Additionally, collection depth of these two techniques is significantly different. Thus we will discuss the spatial and temperature resolution of these two methods.

For the Raman measurements in a confocal mode, the scattered signal is collected from the GaN layer only within a depth of about 1-2  $\mu\text{m}$  while using a high numerical aperture lens. Laterally the spatial resolution of Raman measurement is defined by the width of the light intensity distribution inside the laser focus spot, Airy disk. Comparing results of the thermal simulations and the shape of experimental temperature profile obtained by the Raman method (Fig. 3) confirms that the experimental resolution is close to that predicted from the diffraction limit which is  $\sim 0.5 \mu\text{m}$  for a 488 nm laser light. However large area scans using the Raman method often require a considerable amount of time, as systems has to dwell for several seconds at each measurement spot.

Accuracy of the temperature obtained in Raman measurement depends on the smallest resolvable shift of a phonon mode in the spectrum which can be reliably determined. For instance for the  $E_2(\text{high})$  mode of GaN it corresponds to about  $\pm 5\text{-}10 \text{ }^\circ\text{C}$  at  $100 \text{ }^\circ\text{C}$ . This accuracy improves as the temperature increases, since the temperature gradient of phonon frequency dependence increases with temperature.

Temperature accuracy of the IR technique can approach milliKelvin, when the investigated material has emissivity close to a black body, 0.9-1 [6]. However, for materials with very low emissivity values  $<0.1$ , such as metal contacts, an accurate temperature determination is problematic due to the very low level of actual thermal emission [8]. For infrared imaging operating in the 2-5.5  $\mu\text{m}$  range spatial resolution is diffraction limited to about 3-6  $\mu\text{m}$  [6]. This results in lateral averaging over areas with different temperatures if the size of the hot spot is smaller than 1-2 microns. As a result it leads to an underestimation of the true device peak temperature (Fig. 2 and 3).

In the areas where metal contacts do not cover the surface the measured temperature is close to room ambient (Fig. 2a). For a transparent to IR radiation material, contributions from the whole collection cone of the IR objective lens have to be considered together with reflections of the IR light at interfaces. Effectively it means that for these areas the temperature of the metal heat sink on

the other side of the device is measured (Fig 2a, blue color in the image). This is in contrast to areas covered by metal contacts, 10-15  $\mu\text{m}$  away from the active area, where IR thermography shows a temperature which is close to the result obtained with Raman and simulations (Fig. 2 and 3). Here metal contacts reflect the IR signal towards the detector decreasing the contribution to the acquired signal from transmitted light. Thus in IR thermography materials that are IR-transparent can show a temperature significantly lower, than the surface temperature.

Thus, in order to investigate these limitations further we performed measurements on AlGaIn/GaN TLM test structures fabricated on the same die adjacent to the test transistor, which have ohmic contacts with 20  $\mu\text{m}$  spacing and no gate (Fig. 4 insert). This allows us to exclude the influence of diffraction limited lateral resolution. Due to uniform electrical field distribution in these structures size of the heater region is about 15-20  $\mu\text{m}$ , which is large enough to obtain an IR image without significant influence of lateral temperature averaging. To prevent IR light being collected from various depths in the transparent areas of the circuit, the TLM structure was covered with a layer of a black paint with a thickness of about 10-20  $\mu\text{m}$ . This is a standard method used in IR thermography to improve the accuracy of the temperature measurement in inhomogeneous structures.

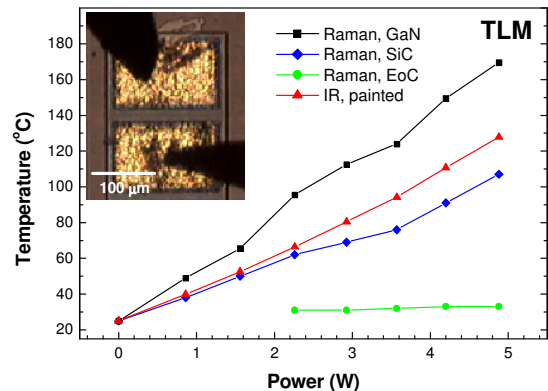


Figure 4. Temperature in the middle of the 20 $\mu\text{m}$  contact gap of the AlGaIn/GaN TLM vs. applied bias. Raman data for GaN, SiC top surface and edge of chip temperature are shown. IR temperature measured on the TLM covered by non transparent black paint layer is also displayed. Insert shows optical image of the TLM structure and contact probes.

Results of IR and Raman temperature measurements on the TLM structure under bias are shown in the Fig. 4. In this case measurements were done from the top side of the device structure. Only areas between metal contacts are optically available in the Raman experiments (no paint on the device during the Raman measurement). Since the temperature profile between the contacts of the TLM structure is rather flat we monitored the temperature of the structure in the middle of the contact gap (Fig. 4). Although the paint layer restricts the measurement depth and, therefore, improves the accuracy of the IR measurement for

IR-transparent devices, the temperature from the IR experiment was still lower than the GaN temperature measured by Raman. Since the measured IR temperature was considerable higher than the temperature of the heat sink and SiC substrate (Fig. 4), this temperature underestimation is possibly related to the temperature gradient in the thick paint layer and poor thermal contact between the paint layer and the device surface. We note that painting potentially risks surface contamination of the device especially at high temperatures and so may be destructive. Therefore a combination of IR thermography for fast assessment of the hot spot location and Raman spectroscopy to retrieve the absolute temperature has great advantages and offers a fast, accurate and non-contact way to monitor device temperatures during operation.

To show that the developed system offers a generic approach, i.e. can be applied on other material systems, we analyzed the temperature rise of a 6x120  $\mu\text{m}$  multi-finger GaAs pHEMT under bias. A sawn die with device structures was mounted on a copper heat sink for the measurements. The result of Raman temperature measurements in the close vicinity (0.5  $\mu\text{m}$ ) to the pHEMT finger at different power levels is shown in Figure 5. Using the Peltier heating stage, self-heating in the device can be monitored at different background temperatures, allowing the system to simulate different working environments.

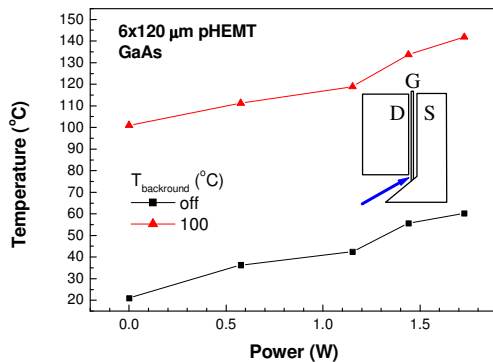


Figure 5. Temperature of a GaAs pHEMT close to the finger (arrow) measured by Raman at different power levels and different background heating conditions: without background heating and with 100 °C applied to a heat sink by Peltier heater stage.

## CONCLUSIONS

We monitored the temperature rise in AlGaIn/GaN device structures due to self-heating using a combined IR/Raman approach. IR thermography is a fast technique to identify the location of hot spots in the device under bias, however accurate temperature determination is difficult. Limited lateral resolution and lack of depth sensitivity leads to underestimation of actual temperature in the device. Confocal Raman spectroscopy offers high submicron spatial resolution combined with micron depth resolution and thus

is much more suitable to obtain accurate temperatures of semiconductor devices. However due to its slow speed it is typically limited to the analysis of small areas of the device. Therefore, it is useful to combine these two methods to achieve fast overview assessment and accurate temperature determination for the analysis of self-heating in device structures. This is also a generic approach, which can be applied to other material systems, such as GaAs.

## ACKNOWLEDGEMENTS

Bristol would like to acknowledge support from EPSRC and QinetiQ Ltd. QinetiQ Ltd was supported by the ES Domain of the UK Ministry of Defense.

## REFERENCES

- [1] Y. F. Wu, A. Saxler, M. Moore, R. P. Smith, S. Sheppard, P. M. Chavarkar, T. Wisleder, U. K. Mishra, P. Parikh, *Electron Device Letter*, IEEE **45**, 117 (2004).
- [2] S. Rajasingam, J. W. Pomeroy, M. Kuball, M. J. Uren, T. Martin, D. C. Herbert, K. P. Hilton, R. S. Balmer, *Electron. Device Letters*, IEEE **25**, 456 (2004).
- [3] M. Kuball, S. Rajasingam, A. Sarua, M. J. Uren, T. Martin, B. T. Huges, K. P. Hilton, R. S. Balmer, *Appl. Phys. Lett.* **82**, 124 (2003).
- [4] M. Kuball, J. M. Hayes M. J. Uren, T. Martin, J. C. H. Birbeck, R. S. Balmer, B. T. Huges, *Electron. Device Letters*, IEEE **23**, 7 (2002).
- [5] D. L. Blackburn, *Semiconductor Thermal Measurement and Management Symposium*, 2004 Twentieth Annual IEEE, pp. 70-80, 2004.
- [6] G. C. Albright, J. A. Stump, J. D. McDonald, and H. Kaplan, *Proc. SPIE Thermosense XXI*, **3700**, 24, 1999.
- [7] D. D. Griffin, *Applied Optics* **7**, 1749 (1968).
- [8] P. W. Webb, *Proc. Inst. Electr. Eng.* **138**, 390 (1991).

## ACRONYMS

DoF: Depth of Field/Focus

HEMT: High Electron Mobility Transistor

HFET: Heterojunction Field Effect Transistor

IR: Infrared

LN<sub>2</sub>: Liquid Nitrogen

NA: Numerical Aperture

RF: Radio Frequency

TLM: Transfer Length Measurement

WD: Working Distance